U.S. DEPARTMENT OF ENERGY | Office of Science

NSTX-U

The ins and outs of modelling vertical displacement events

D.Pfefferlé[1]

N.Ferraro [1] **S.Jardin**[1] **C.E.Myers**[1] **I.Krebs**[1] **A.Bhattacharjee**[1]

[1] *Princeton Plasma Physics Laboratory, Princeton NJ, USA*

59th Annual Meeting of the APS Division of Plasma Physics
October 23–27 2017, Milwaukee, Wisconsin, USA

PPPL

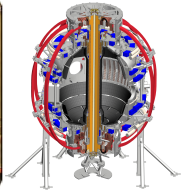

VDEs result in largest forces among disruptive events

- Tokamaks are prone to **disruptions** [Hender et al., 2007]
  - disruption database show wide range of behaviours *(see top figure)*
- Vertical Displacement Event (VDE) is when positional control is lost and unstable elongated plasma drifts into vessel
  - abrupt release of thermal and magnetic energy
  - currents, forces, stresses, heat loads ⇒ severe **structural damage**
  - worse if toroidal asymmetry and rotation (peaking, resonance, *bottom figure*)

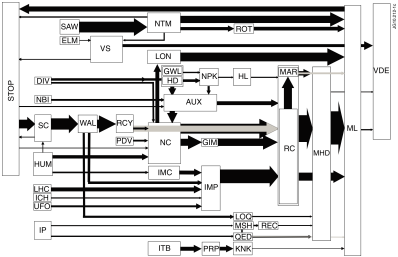

Courtesy of [de Vries et al., 2011]

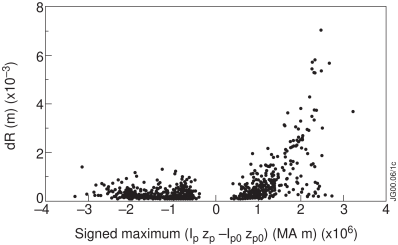

Courtesy of [Riccardo et al., 2000]

Origin of wall currents varies during multi-phase hot VDE

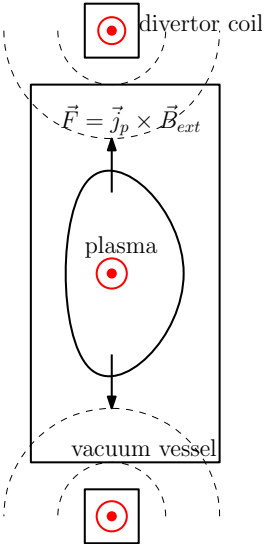

- drifting phase
  - conducting vessel only allows flux change on resistive timescales
  - **"slow"**, $\tau_{VDE} \gg \tau_A$, even in 3D [Zakharov, 2008]
  - **opposing currents** either in wall or leading halo
- contact phase
  - slow transfer of flux from core to halo+wall, peel off of flux-surfaces
    - $q_{edge} \propto a^2/I(a)$ tends to drop
    - kink instabilities as $q_{edge} \lesssim 2$
    - edge currents trigger peeling modes, filaments [Ebrahimi, 2017]
  - induced currents from rapidly cooling plasma
    - resistivity increases due to thermal quench
    - fast plasma current quench drives currents in halo (force-free) and wall, q_{edge} rises
    - danger of runaway electrons in large devices

Origin of wall currents varies during multi-phase hot VDE

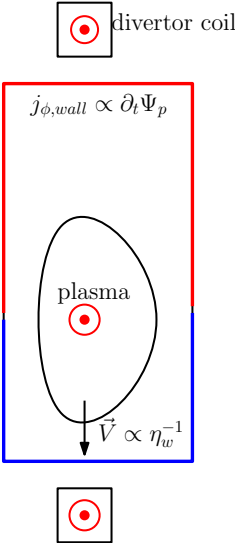

- drifting phase
  - conducting vessel only allows flux change on resistive timescales
  - **"slow"**, $\tau_{VDE} \gg \tau_A$, even in 3D [Zakharov, 2008]
  - **opposing currents** either in wall or leading halo
- contact phase
  - slow transfer of flux from core to halo+wall, peel off of flux-surfaces
    - $q_{edge} \propto a^2/I(a)$ tends to drop
    - kink instabilities as $q_{edge} \lesssim 2$
    - edge currents trigger peeling modes, filaments [Ebrahimi, 2017]
  - induced currents from rapidly cooling plasma
    - resistivity increases due to thermal quench
    - fast plasma current quench drives currents in halo (force-free) and wall, q_{edge} rises
    - danger of runaway electrons in large devices

Origin of wall currents varies during multi-phase hot VDE

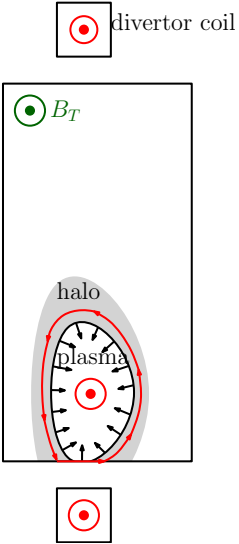

- drifting phase
  - conducting vessel only allows flux change on resistive timescales
  - **"slow"**, $\tau_{VDE} \gg \tau_A$, even in 3D [Zakharov, 2008]
  - **opposing currents** either in wall or leading halo
- contact phase
  - slow transfer of flux from core to halo+wall, peel off of flux-surfaces
    - $q_{edge} \propto a^2/I(a)$ tends to drop
    - kink instabilities as $q_{edge} \lesssim 2$
    - edge currents trigger peeling modes, filaments [Ebrahimi, 2017]
  - induced currents from rapidly cooling plasma
    - resistivity increases due to thermal quench
    - fast plasma current quench drives currents in halo (force-free) and wall, q_{edge} rises
    - danger of runaway electrons in large devices

Need for realistic modelling of 3D effects during hot VDEs

Extensive modelling

1. axisymmetric Grad-Shafranov coupled to wire models of wall
   - TSC [Jardin et al., 1986; Miyamoto et al., 2012], DINA [Khayrutdinov and Lukash, 1993], MAXFEA [Miki et al., 2001]
2. very detailed models of the wall, but ad-hoc plasma physics
   - VALEN [Bialek et al., 2001], CARIDDI [Albanese et al., 2015], [Roccella et al., 2008]
3. resistive MHD simulations at low Lundquist number, poor separation with Alfvén timescales
   - M3D [Strauss et al., 2014], CTD [Aydemir, 2000]

Full non-linear 3D modelling using resistive MHD code M3D-C1

- minimal intervention to influence hot VDE history (plasma current, sources)
  - driving mechanisms, chain of events, timing of various effects, sensitivity to parameter change
- realistic timescales and parameters via computationally challenging simulations
- assessment of halo/wall currents and wall forces
  - qualitative comparison with shunt tile diagnostics

M3D-C1 has unique capabilities for modelling VDEs

- XMHD [Breslau et al., 2009; Ferraro et al., 2016]
  - continuity, momentum, energy
  - Faraday, Ampère, Ohm
- resistive wall, $\partial_t \boldsymbol{B} = -\nabla \times (\eta_{wall} \boldsymbol{j})$
- vacuum, $\boldsymbol{j} = 0$
- ideal boundary (perfect conductor)
- PF coils (static)

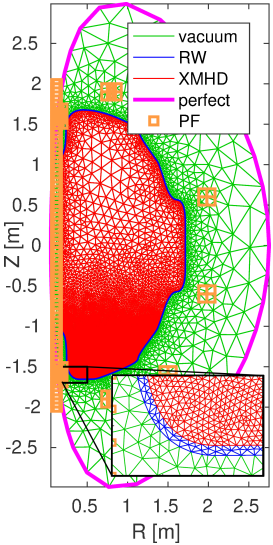

$$\partial_t n + \nabla \cdot (n\boldsymbol{v}) = -D\nabla^2 n$$

$$mn\frac{d\boldsymbol{v}}{dt} = \boldsymbol{j} \times \boldsymbol{B} - \nabla p - \nabla \cdot \boldsymbol{\Pi}$$

$$\frac{dp}{dt} + \Gamma p \nabla \cdot \boldsymbol{v} = (\Gamma - 1)(\eta j^2 - \nabla \cdot \boldsymbol{q} - \boldsymbol{\Pi} : \boldsymbol{v})$$

with $\boldsymbol{q} = -\kappa_\perp \nabla T - \kappa_{||} \boldsymbol{bb} \cdot \nabla T$,
$\boldsymbol{\Pi} = \mu(\nabla \boldsymbol{v} + \nabla \boldsymbol{v}^T) + \lambda(\nabla \cdot \boldsymbol{v})\boldsymbol{I}$, $T = p/n$,
$\eta \propto T^{-3/2}$ (Spitzer)

$$\partial_t \boldsymbol{B} = \nabla \times [\boldsymbol{v} \times \boldsymbol{B} - \eta \boldsymbol{j}]$$

$$\nabla \times \boldsymbol{B} = \mu_0 \boldsymbol{j}$$

M3D-C1 has unique capabilities for modelling VDEs

- XMHD [Breslau et al., 2009; Ferraro et al., 2016]
  - continuity, momentum, energy
  - Faraday, Ampère, Ohm
- resistive wall, $\partial_t \boldsymbol{B} = -\boldsymbol{\nabla} \times (\eta_{wall} \boldsymbol{j})$
- vacuum, $\boldsymbol{j} = 0$
- ideal boundary (perfect conductor)
- PF coils (static)

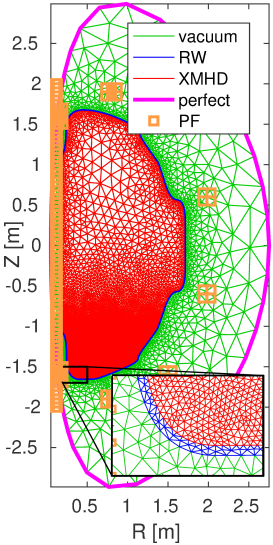

- key features
  - finite-thickness **axisymmetric** resistive wall
  - **anisotropic** unstructured mesh for finite-element (weak) **C1** solution
  - cubic spline on **48** planes for **3D**
  - **implicit** time-stepping allows simulations on RW timescales
- limiting assumptions
  - halo is a cold, low density, resistive plasma (choice of T_{halo})
  - static external fields

Experimental traces serve as modelling targets

Reproduce NSTX #139536

[Gerhardt et al., 2012; Breslau, 2015]

- VDE phases and timescales
  - **slow** vertical motion $\tau_{VDE} \sim 50ms$, largely exponential
  - **rapid** $\tau_{CQ} \sim 5ms$ current quench begins at wall contact
  - relaxation of wall currents $\tau_{LR} \sim 10ms$
- shunt tile $n = 0 \sim n = 1$ throughout current quench

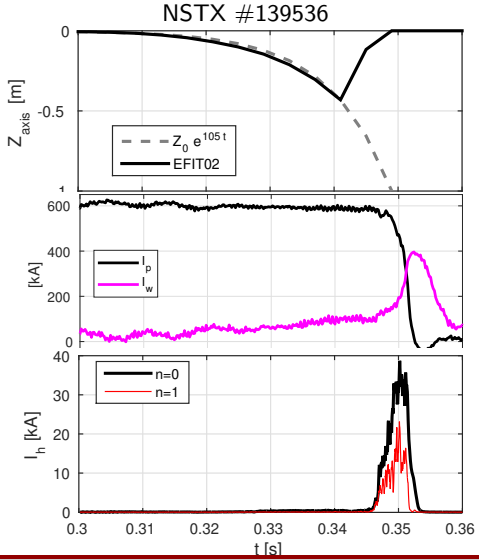

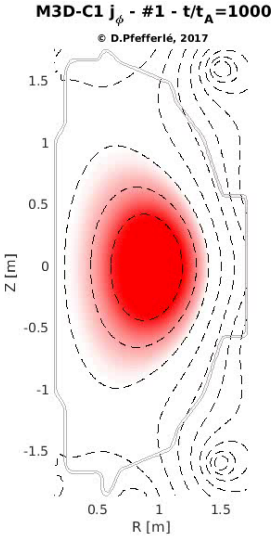

Wall resistivity defines characteristic VDE duration

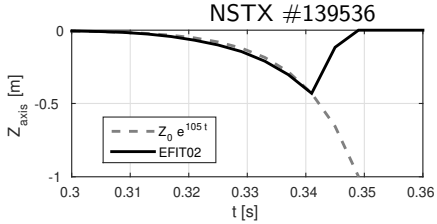

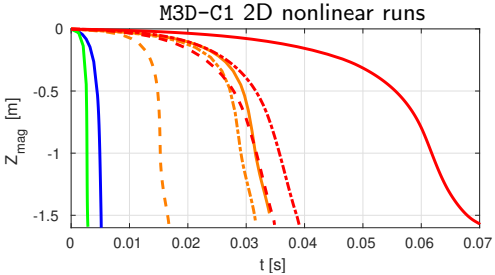

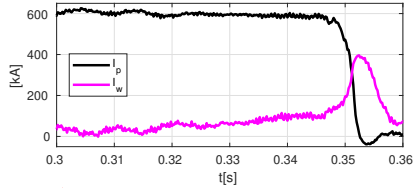

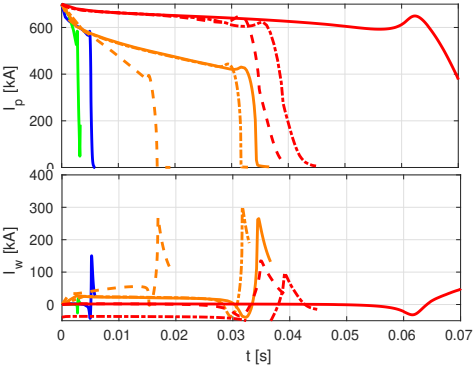

$\eta_w = 4.9\times10^{-4}$, 4.9×10^{-5}, 5.8×10^{-6}, 1.9×10^{-6} Ωm

Halo temperature has notable impact on VDE evolution

- VDE characteristic time $\gamma_{VDE} \propto \eta_{wall}$
- Open field-line plasma
  - thermal contact with wall (high $\kappa_{||}$)
  - line-tied to wall on Alfvénic timescales
- $T_{halo} = \frac{p_{edge}}{n_{edge}}$, boundary condition
  - to avoid negative overshoot (advection), $p_{edge}/p_0 \gtrsim 10^{-5} \Rightarrow n_{edge}/n_0 \sim 10^{-2}$
  - $T_{halo} = 25eV$ and $\eta_{halo} \sim 1.4 \times 10^{-5} \Omega m$
  - cross-section of open field-line region is large $\Rightarrow$ **halo resistance** competes with wall
- **Workaround**: compute Spitzer resistivity by

$$\eta(\boldsymbol{x}) = \frac{\eta_0}{(T_e(\boldsymbol{x}) - T_{\text{offset}})^{3/2}}$$

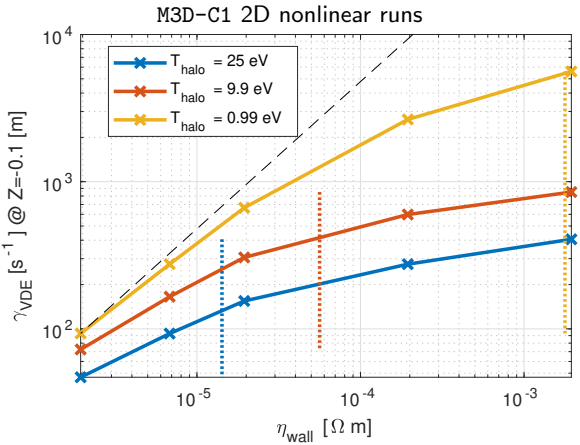

Halo temperature has notable impact on VDE evolution

- VDE characteristic time $\gamma_{VDE} \propto \eta_{wall}$
- Open field-line plasma
  - thermal contact with wall (high $\kappa_{||}$)
  - line-tied to wall on Alfvénic timescales
- $T_{halo} = \frac{p_{edge}}{n_{edge}}$, boundary condition
  - to avoid negative overshoot (advection), $p_{edge}/p_0 \gtrsim 10^{-5} \Rightarrow n_{edge}/n_0 \sim 10^{-2}$
  - $T_{halo} = 25eV$ and $\eta_{halo} \sim 1.4 \times 10^{-5} \Omega m$
  - cross-section of open field-line region is large $\Rightarrow$ **halo resistance** competes with wall
- **Workaround**: compute Spitzer resistivity by

$$\eta(\boldsymbol{x}) = \frac{\eta_0}{(T_e(\boldsymbol{x}) - T_{\text{offset}})^{3/2}}$$

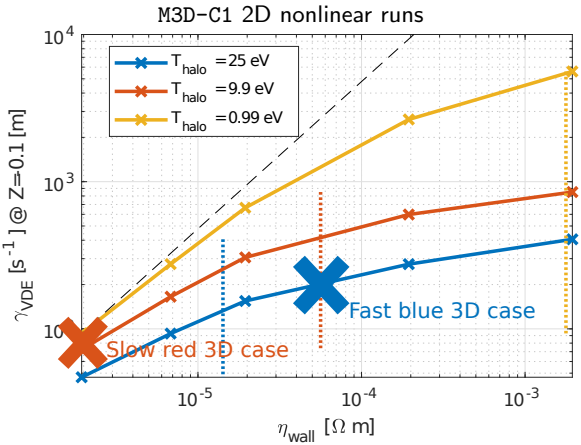

3D nonlinear simulations capture rich physics

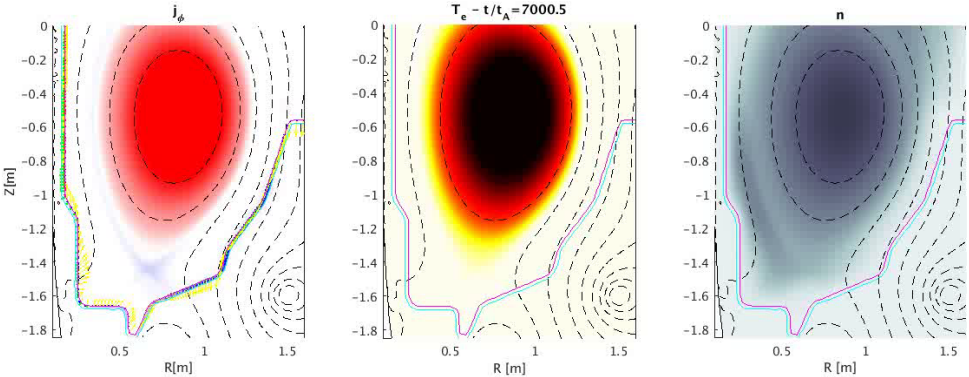

- halo region plays active role
  - opposing induced currents (divertor)
  - broad contact with wall
  - late onset of 3D modes, **stabilizing** halo

- Fast blue case
  - $\eta_{wall} = 4.9 \times 10^{-5}$ Ωm, short τ_{VDE}
  - high $T_{halo} = 25$ eV

3D nonlinear simulations capture rich physics

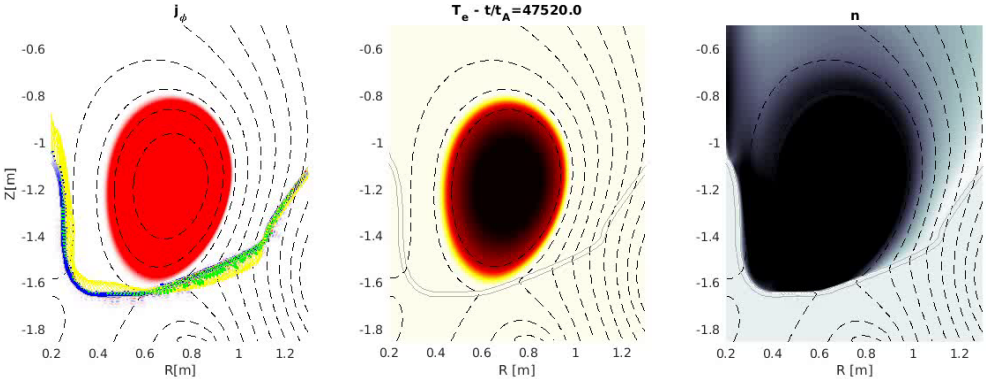

- less active halo
  - thin halo, narrow contact point with wall
  - 3D edge modes triggered immediately
  - filamentation, vacuum bubbles [Rosenbluth et al., 1976]

- Slow red case
  - $\eta_{wall} = 1.9 \times 10^{-6}$ Ωm, long τ_{VDE}
  - low $T_{halo} = 9$ eV

Isocontours of $\Psi_p - < \Psi_p >$ reveal toroidal modes

- Slow red case
  - $\eta_{wall} = 1.9 \times 10^{-6}$ Ωm
  - low $T_{halo} = 9$ eV
- figure caption
  - poloidal cuts at $\phi = 0, \pi$
  - isocontours at $\pm\tilde{\Psi}_{p,max}/2$
  - transparency scales with mode amplitude
- $n = 6$ peeling-ballooning collapsing into $n = 2$ global mode
- low degree of kinking

Penetrating edge modes responsible for initiating current quench

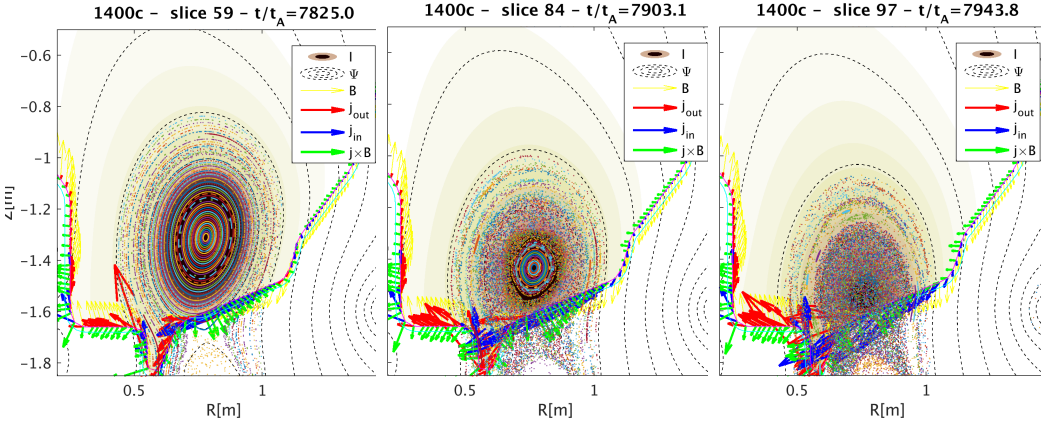

- stochastic field-lines $\Rightarrow$ efficient heat transport via parallel conductivity $\kappa_{||}$
- rapid cooling (cold wall) $\rightarrow$ increase in Ohmic dissipation
- only from 3D (effective 2D model?)

Onset of 3D modes precipitates current quench

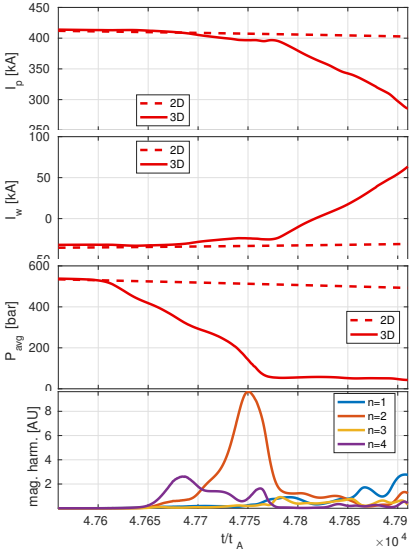

- Slow red case
  - $\eta_{wall} = 1.9 \times 10^{-6}$ Ωm, long τ_{VDE}
  - low $T_{halo} = 9$ eV
- 3D evolution identical to 2D until presence of large amplitude toroidal modes
- observations
  1. degradation of thermal energy (P_{avg})
  2. current density flattening ⇒ drop in internal inductance ⇒ steady plasma current $LI_p = \Psi_p$
  3. resistivity increase as plasma stops cooling ⇒ decay of plasma current ⇒ current transfer to wall

Normal wall current inherit 3D patterns from imploding plasma

normal currents on wall (total)

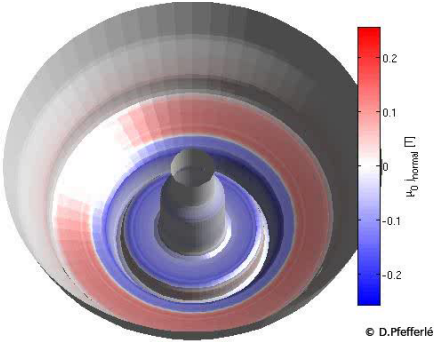

Fast blue case

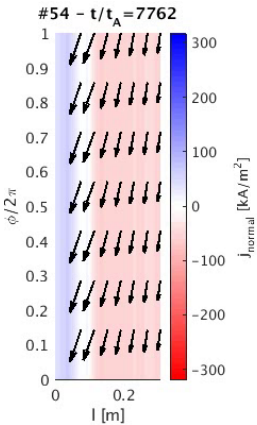

Slow red case

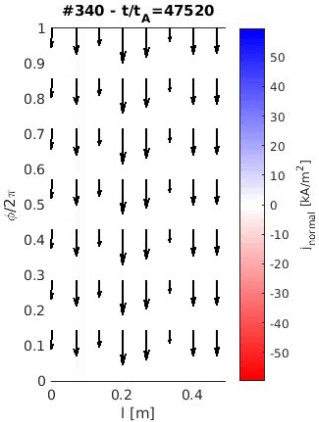

toroidal (arrows) and normal (colour) currents on divertor

- pattern rotation
  - zero global momentum (no net rotation)
  - sheared rotation from peeling of q
  - amplitude qualitatively matches experimental shunt tiles

Conclusions

- Modelling of NSTX **hot** VDEs using `M3D-C1`
  - realistic τ_{VDE}, τ_{CQ} and τ_{LR} timescales
  - parameter scans with 2D nonlinear simulations and assessment of halo temperature on τ_{VDE}
  - **heavy** 3D nonlinear simulations deployed for two choices of T_{halo}
- T_{halo} affects timing (onset) of 3D modes (VDE evolution)
  - high T_{halo}: stabilising effect $\Rightarrow$ slower current quench
  - low T_{halo}: immediate onset of edge modes $\Rightarrow$ rapid degradation of thermal energy
    - halo width (contact area) could be determined experimentally $\Rightarrow$ increase **poloidal resolution** of shunt tiles
- break-up of flux-surfaces (3D effect) responsible for rapid thermal quench
  - inward penetration of modes, initially high-n, cascading to low-n
  - field-line stochastisation $\Rightarrow$ rapid cooling $\Rightarrow$ precipitates current quench
  - time-evolving non-axisymmetric patterns are complex
    - shearing, merging, rotation is unclear $\Rightarrow$ increase **toroidal resolution** of shunt tiles

Computational boundary does not affect VDE

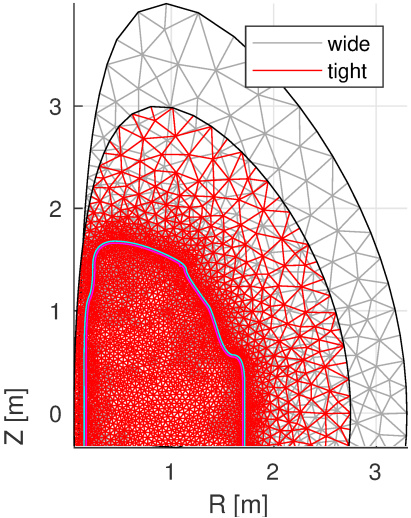

- computational boundary is a perfect conductor
- $< 1\%$ effect on non-linear 2D evolution for highest wall resistivity and fastest VDE

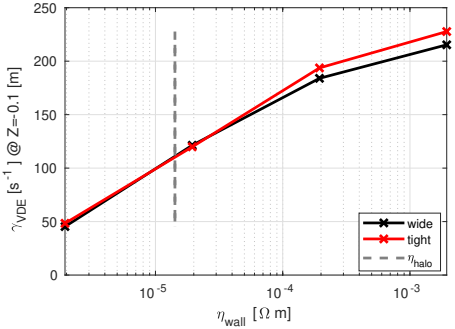

Induced wall currents supported by few mesh points

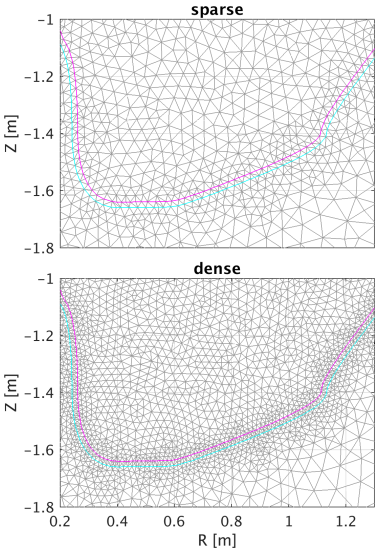

- skin depth $\delta = \sqrt{2\eta_w/\gamma_{VDE}\mu_0} \gtrsim 10cm$
- currents are well resolved in resistive wall despite small thickness

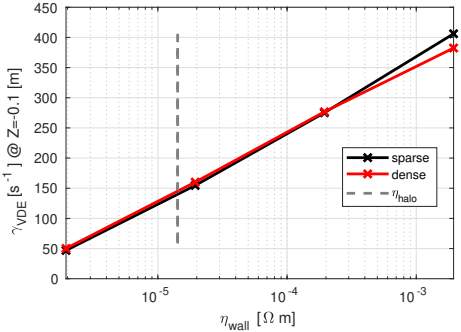

Bibliography I

T. Hender, J. Wesley, J. Bialek, A. Bondeson, A. Boozer, R. Buttery, A. Garofalo, T. Goodman, R. Granetz, Y. Gribov, et al., Nuclear Fusion **47**, S128 (2007).

P. de Vries, M. Johnson, B. Alper, P. Buratti, T. Hender, H. Koslowski, V. Riccardo, and J.-E. Contributors, Nuclear Fusion **51**, 053018 (2011).

V. Riccardo, S. Walker, and P. Noll, Plasma Physics and Controlled Fusion **42**, 29 (2000).

L. E. Zakharov, Physics of Plasmas **15**, 062507 (2008).

F. Ebrahimi, Physics of Plasmas **24**, 056119 (2017).

Bibliography II

S. Jardin, N. Pomphrey, and J. Delucia, Journal of Computational Physics **66**, 481 (1986), ISSN 0021-9991.

S. Miyamoto, M. Sugihara, K. Shinya, Y. Nakamura, S. Toshimitsu, V. Lukash, R. Khayrutdinov, T. Sugie, Y. Kusama, and R. Yoshino, Fusion Engineering and Design **87**, 1816 (2012).

R. Khayrutdinov and V. Lukash, Journal of Computational Physics **109**, 193 (1993), ISSN 0021-9991.

Bibliography III

N. Miki, M. Verrecchia, P. Barabaschi, A. Belov, S. Chiocchio, F. Elio, K. Ioki, S. Kikuchi, V. Kokotkov, J. Ohmori, et al., Fusion Engineering and Design **58**, 555 (2001), ISSN 0920-3796.

J. Bialek, A. H. Boozer, M. E. Mauel, and G. A. Navratil, Physics of Plasmas **8**, 2170 (2001).

R. Albanese, B. Carpentieri, M. Cavinato, S. Minucci, R. Palmaccio, A. Portone, G. Rubinacci, P. Testoni, S. Ventre, and F. Villone, Fusion Engineering and Design **94**, 7 (2015), ISSN 0920-3796.

Bibliography IV

M. Roccella, A. Marin, F. Lucca, and M. Merola, Fusion Engineering and Design **83**, 1625 (2008), ISSN 0920-3796, proceedings of the Eight International Symposium of Fusion Nuclear Technology.

H. Strauss, L. Sugiyama, R. Paccagnella, J. Breslau, and S. Jardin, Nuclear Fusion **54**, 043017 (2014).

A. Y. Aydemir, Joint Varenna-Lausanne International Workshop on Theory of Fusion Plasmas (2000).

J. Breslau, N. Ferraro, and S. Jardin, Physics of Plasmas **16**, 092503 (2009).

Bibliography V

N. M. Ferraro, S. C. Jardin, L. L. Lao, M. S. Shephard, and F. Zhang, Physics of Plasmas **23**, 056114 (2016).

S. Gerhardt, J. Menard, S. Sabbagh, and F. Scotti, Nuclear Fusion **52**, 063005 (2012).

J. Breslau, TSDW 15 (2015).

M. N. Rosenbluth, D. A. Monticello, H. R. Strauss, and R. B. White, The Physics of Fluids **19**, 1987 (1976).